Electronic Supplementary Material (ESI) for Dalton Transactions.
This journal is © The Royal Society of Chemistry 2015

Immobilisation of a molecular epoxidation catalyst on UiO-66 and -67: effect of pore size on catalyst activity and recycling

Marlene Kaposi, Mirza Cokoja,* Christine H. Hutterer, Simone A. Hauser, Alexander Pöthig, Wolfgang A. Herrmann and Fritz E. Kühn*

Chair of Inorganic Chemistry/ Molecular Catalysis, Catalysis Research Center and Department of Chemistry, Technische Universität München, Lichtenbergstraße 4, D-85747 Garching bei München, Germany. E-mails: mirza.cokoja@tum.de, fritz.kuehn@ch.tum.de

Electronic Supporting Information

Table of contents

1 Characterisation

1.1 Powder X-ray diffraction

Powder X-ray diffraction was carried out using a Stoe Stadi P diffractometer operated with $CuK_{\alpha 1}$ radiation (λ = 1.5406 Å) and a Ge(111) monochromator in transmission mode.

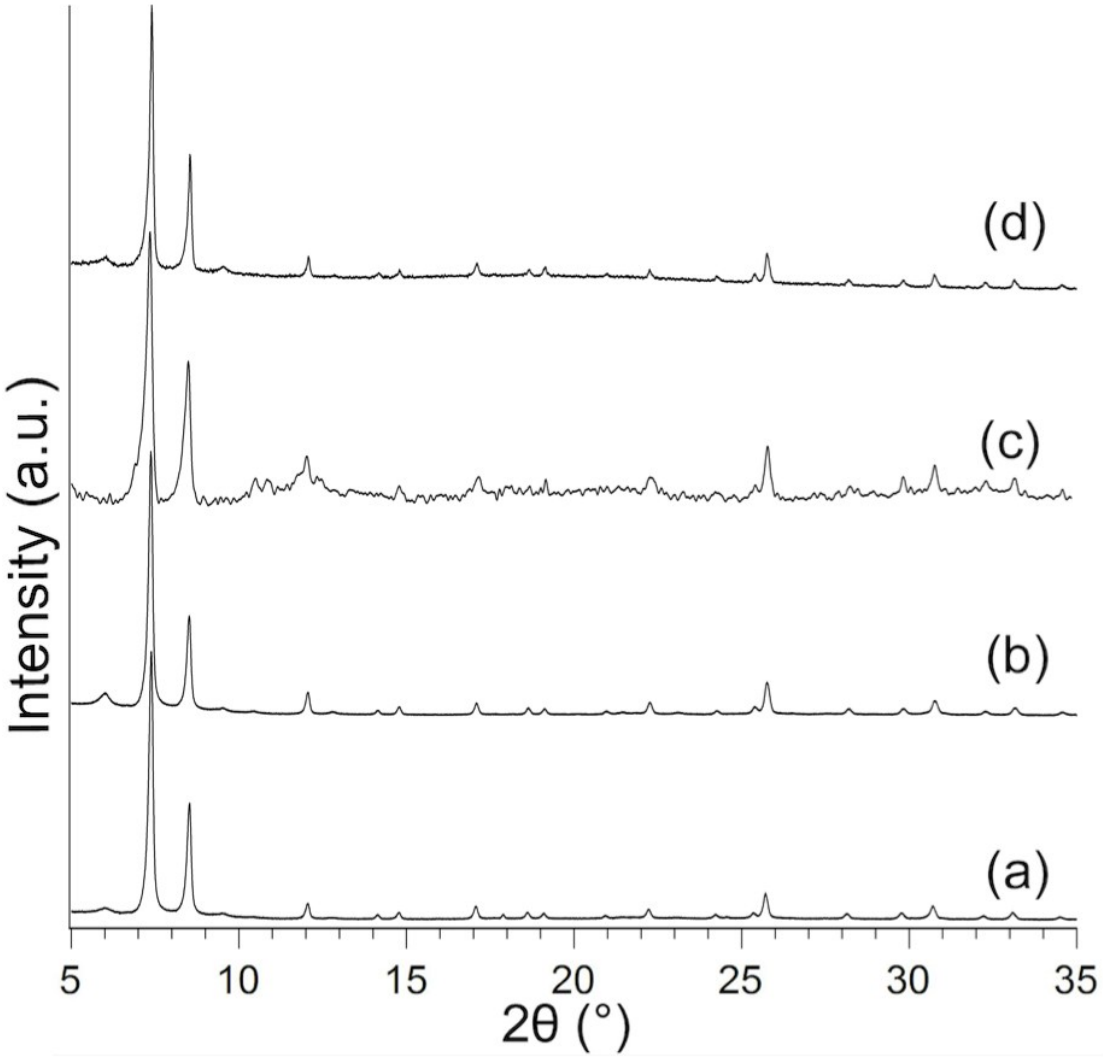

Fig. S1. PXRD patterns of (a) UiO-66, (b) UiO-66-SI, (c) Mo@UiO-66 and (d) Mo@UiO-66 after catalysis.

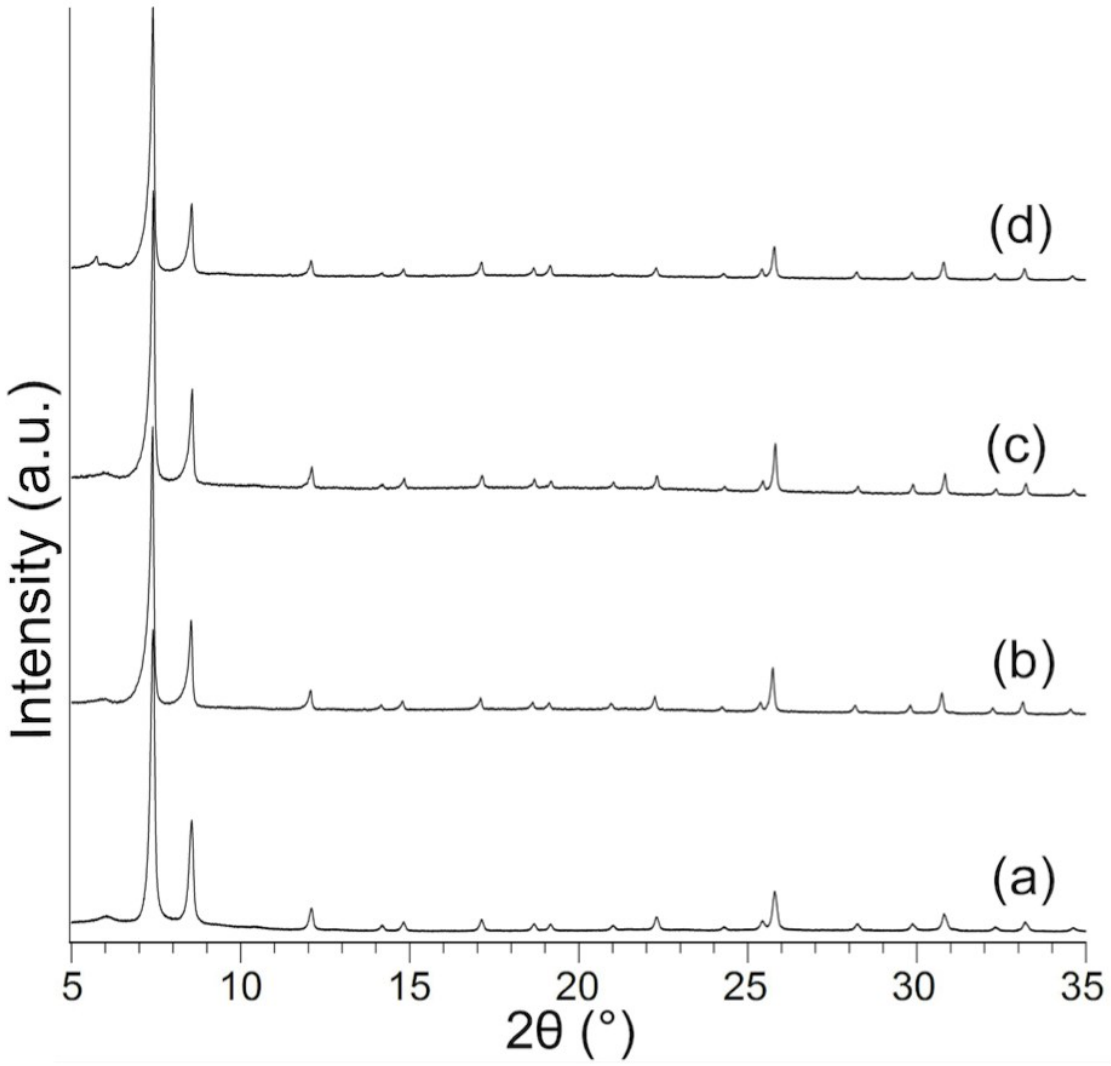

Fig. S2. PXRD patterns of (a) UiO-66-mixed, (b) UiO-66-SI-mixed, (c) Mo@UiO-66-mixed and (d) Mo@UiO-66-mixed after catalysis.

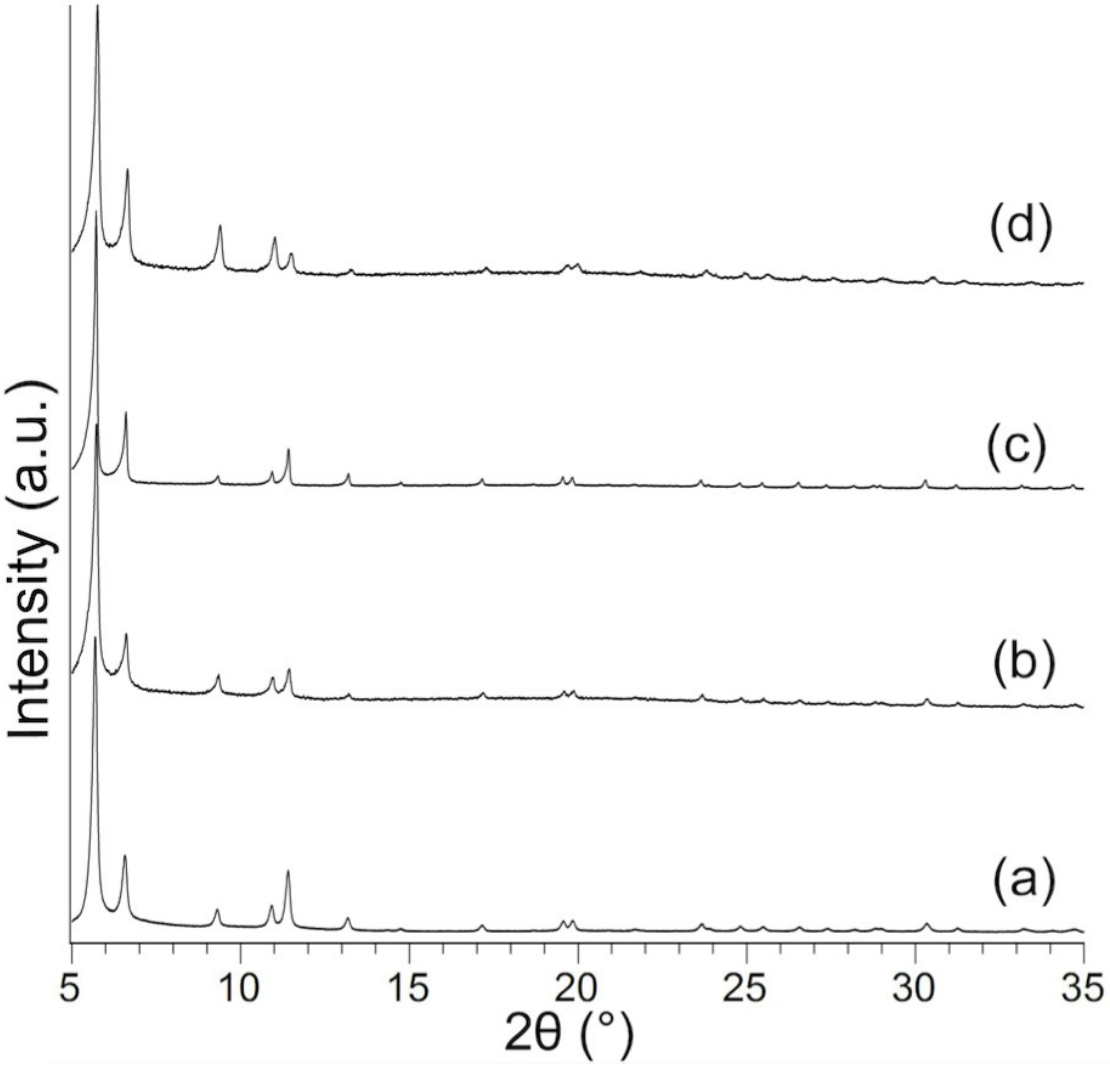

Fig. S3. PXRD patterns of (a) UiO-67, (b) UiO-67-SI, (c) Mo@UiO-67 and (d) Mo@UiO-67 after catalysis.

1.2 X-ray single crystal diffraction

Table S1. Crystallographic data for compounds UiO-67-NH_2 and [MoO_2(acac)(PhN=C-PhO)].

	UiO-67-NH_2	**[MoO_2(acac)(PhN=C-PhO)]**
Formula	$C_{42}H_{24}N_3O_{16}Zr_3$	$C_{18}H_{17}MoNO_5$
fw	1100.32	423.27
Colour/habit	yellow prism	yellow block
Cryst. dimensions (mm^3)	0.25 x 0.29 x 0.35	0.25 x 0.31 x 0.31
Crystal system	cubic	triclinic
Space group	$Fm\bar{3}m$	$P\bar{1}$
a, Å	26.7882(6)	7.0807(1)
b, Å	26.7882(6)	9.4110(1)
c, Å	26.7882(6)	14.0768(2)
α, deg	90	93.622(1)
β, deg	90	99.297(1)
γ, deg	90	111.590(1)
V, $Å^3$	19223.4(13)	853.04(2)
Z	8	2
T, K	123(2)	123
D_{calcd}, g cm^{-3}	0.760	1.648
μ, mm^{-1}	0.353	0.797
F(000)	4360	428
θ range, deg	1.32 – 25.38	2.35 – 25.44
Index ranges (h, k, l)	-32 – 31, ±32, ±32	±8, ±11, ±16
No. of rflns collected	160563	24703
No. of independent rflns/R_{int}	951/0.0344	3145/0.0258
No. of observed rflns (I>2σ(I))	914	3020
No. of data/restraints/parameters	951/26/52	3145/0/228
R1/wR2 (I>2σ(I))[a]	0.0481/0.1378	0.0166/0.0421
R1/wR2 (all data)[a]	0.0495/0.1396	0.0176/0.0426
GOF (on F^2)[a]	1.237	1.083
Largest diff peak and hole (e $Å^{-3}$)	0.919/-0.885	+0.255/-0.298

[a] $R1 = \sum(||F_o|-|F_c||)/\sum|F_o|$; $wR2 = \{\sum [w(F_o^2-F_c^2)^2]/ \sum[w(F_o^2)^2]\}^{1/2}$; $GOF = \{\sum[w(F_o^2-F_c^2)^2]/(n-p)\}^{1/2}$

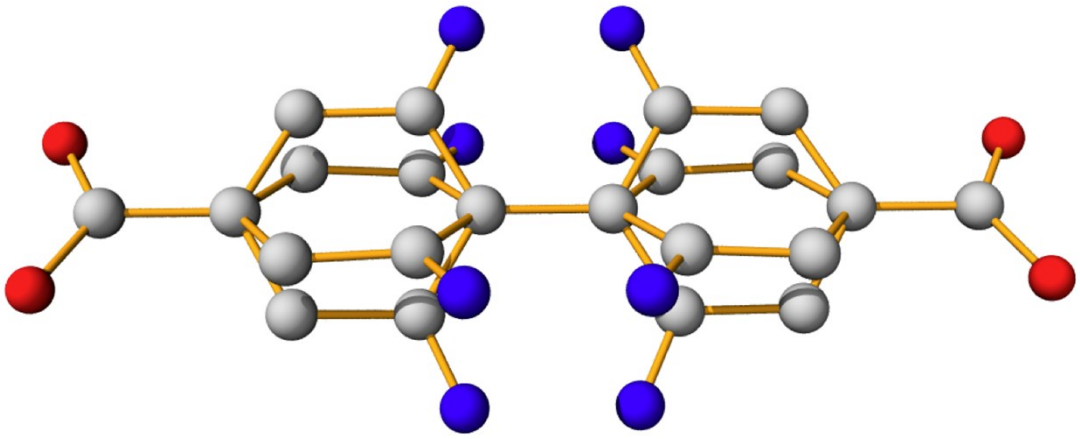

Fig. S4. Disorder of aromatic rings in UiO-67-NH_2 (H atoms omitted for clarity).

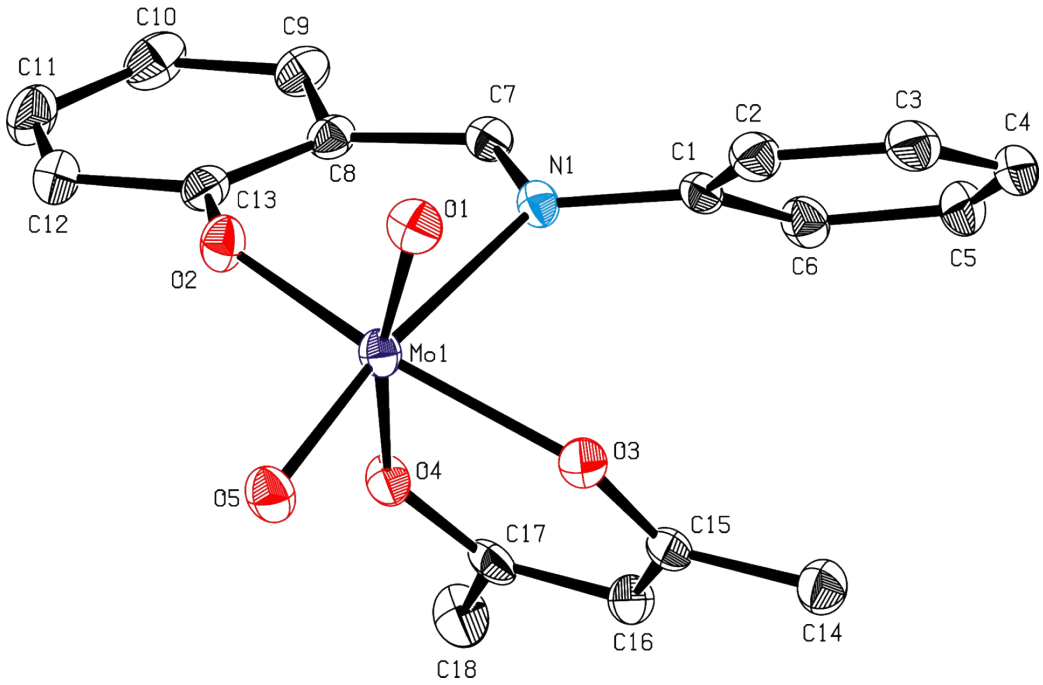

Fig. S5. ORTEP style drawing of [MoO_2(acac)(PhN=C-PhO)] in the solid state. Thermal ellipsoids are drawn at the 50% probability level. Selected bond lengths [Å] and bond angles [°]: Mo1–O1 1.7025(13), Mo1–O2 1.9196(12), Mo1–O3 2.0161(11), Mo1–O4 2.1814(12), Mo1–O5 1.7118(13), Mo1–N1 2.3579(15); O1–Mo1–O2 100.03(6), O1–Mo1–O3 93.53(5), O1–Mo1–O5 104.34(6), O2–Mo1–O4 81.02(5), O2–Mo1–O5 99.71(6), O3–Mo1–O4 80.72(5), O3–Mo1–O5 95.51(5), O1–Mo1–N1 89.37(6), O2–Mo1–N1 80.94(5), O3–Mo1–N1 79.94(5).